MM Science Journal | www.mmscience.eu
ISSN 1803-1269 (Print) | ISSN 1805-0476 (On-line)
Special Issue | TEAM 2024
Transdisciplinary and Emerging Approaches to Multidisciplinary Science
11.9.2024 – 13.9.2024, Ostrava, Czech Republic
DOI: 10.17973/MMSJ.2024_10_2024060

TEAM2024-00001

HEAT TREATMENT FOR MICROSTRUCTURE STABILIZING OF BIOMEDICAL TI-6AL-4V ALLOY FABRICATED BY SELECTIVE LASER MELTING

MINH-THUYET NGUYEN[1*], VAN-TRUNG TRINH[1]

[1]Hanoi University of Science & Technology, School of Materials Science & Engineering, Hanoi, Vietnam

*Corresponding author; e-mail: thuyet.nguyenminh@hust.edu.vn

Abstract
In this study, the microstructural evolution of the microstructure and phase transformation of the biomedical Ti-6Al-4V alloys fabricated by Selective Laser Melting (SLM) at various solution treatment temperatures was investigated in order to achieve the formation and stabilization of (α + β) lamella structure for the final products. Solution heat treatments were conducted at 850℃ for 2.5 hours; at 950℃ or 1020℃ for 1 h and followed by cooling naturally in the oven. The α' martensite in the SLMed samples was transformed from the β phase after heat treatment and finally achieved the uniform (α + β) lamella structure in heat treated samples of Ti-6Al-4V alloys. The dependence of the transformation behavior of the β phase during the solution treatment was determined by the partitioning of α and β stabilizing elements.

Keywords:
SLMed Ti-6Al-4V, Heat Treatment, Microstructure Stabilizing

1 INTRODUCTION

In recent years, the advancement of additive manufacturing techniques has revolutionized the production of biomedical implants, particularly those made from titanium alloys. Among these techniques, Selective Laser Melting (SLM) has emerged as a prominent method for fabricating complex, patient-specific implants with high precision and mechanical properties [Singla 2021]. Titanium alloy Ti-6Al-4V stands out as a preferred material in biomedical applications due to its biocompatibility, corrosion resistance, and mechanical strength [Niinomi 2008].

Based on the phase diagram of the Ti-6Al-V alloy [Peters 2003], the microstructure of Ti-6Al-V can be classified into α, (α + β), and β alloys according to V content, with further subdivision into near-α and near-β alloys. Hence Ti-6Al-4V with 4% of V is classified as (α + β) titanium alloy. In biphasic α + β alloys, two distinctly different microstructures are typically observed, depending on the morphology of the α phase: slab and (equiaxed) sphere [Calignano 2019, Chen 2015]. Titanium alloys characterized by a combination of these microstructures, such as bimodal microstructures or even trimodal microstructures as well as a mixture of coarse and lamellar structures known as biphasic microstructures, can exhibit unique mechanical properties [Chen 2015, Virginia 2013]. However, the as-printed condition of SLM-produced (SLMed) Ti-6Al-4V alloys may not always meet the stringent requirements of biomedical implant microstructure. Thus, the previous studies on the microstructure of SLMed Ti-6Al-4V alloys showed that the SLMed samples exhibited a microstructure consisting predominantly of α' martensite and β phases, and the micro-hardness values were not uniform across different surfaces [Singla 2021, Calignano 2019, Nguyen 2020, Önder 2023, Xu 2015]. The formation of a martensitic microstructure poses a challenge for Ti-6Al-4V produced via SLM for biomedical implants [Xu 2015]. Numerous reports have shown that SLMed Ti6Al4V samples consisting solely of α′ martensite exhibit low ductility, often less than 10% [Niinomi 2008, Virginia 2013, Xu 2015, Vilaro 2011], indicating that the α′ phase is not suitable for biomedical implant applications. Additionally, residual stresses associated with the formation of the martensitic structure α′ lead to decrease mechanical efficiency. The SLM process, characterized by high localized heat input, short interaction time, rapid solidification, and large thermal gradients, induces thermal stresses. It is well recognized that the fatigue performance of SLMed parts can be affected by the residual stresses generated due to the high cooling rate and thermal gradient inherent in the SLM process [Singla 2021, Calignano 2019, Xu 2015, Vilaro 2011, Pederson 2012, Harun 2018]. Moreover, according to ASTM F13-12a and ASTM F2924-14, an implant or SLM microstructure must exhibit a minimum ductility of 10% and contain an alpha (α)-beta (β) dual phase. Therefore, it is imperative to explore methods to transform the microstructure of SLM-produced Ti-6Al-4V from the (α′) phase to the stable (α + β) phase to enhance ductility and mitigate internal residual stresses.

Given the necessity to transform the SLMed Ti-6Al-4V alloy structure from martensite to (α + β) to improve ductility and

reduce internal residual stress, researchers have considered heat treatment as a solution. Heat treatment is the process of heating metal without letting it reach its molten stage, and then cooling the metal in a controlled manner to achieve desired microstructure and mechanical properties. Heat treatment is used to either strengthen metal or make it more malleable, resistant to abrasion, or ductile [Rack 2015]. For the SLMed Ti-6Al-4V alloy, the purpose of heat treatment is to take advantage of increasing heat to form the Tiβ (BCC) structure. At temperatures from 850 °C, the β phase begins to form from α / α' phases, followed by a process of heat preservation and slow cooling in the furnace to prevent the β phase re-converting into martensite α′ [Peters 2003, Calignano 2019, Chen 2015]. Additionally, heat treatment is expected to reduce the defects as pores, cracks, or un-melted powder parts, which appear in Ti-6Al-4V after the SLM process.

Hence, this study aims to investigate the effects of heat treatment on the microstructure and properties of biomedical Ti-6Al-4V alloys manufactured by SLM and achieve the stabilization of the (α + β) phase. Specifically, the research will focus on the changes in the microstructure of SLMed Ti-6Al-4V alloys under various heat treatment parameters, as well as correlating the microstructural changes with mechanical properties such as the hardness of SLM-fabricated Ti-6Al-4V alloys through heat treatment.

2 MATERIALS AND METHODS

The samples were prepared by using the SLM technique from the initial gas-atomized Ti-6Al-4V powders with the particle size below 45 μm. All the samples investigated in this work were built in cubic shapes with dimensions of 10x10x10 mm^3 by using an SLM machine (METALSYS 150) with a non-support part process option. A zig-zag pattern of scanning strategies with a rotation angle of about 67° of the next layer to the previous layer during the SLM process and parameter conditions were shown in Table 1.

The as-built samples were heat treated at 850 °C for 2.5 h, 950 °C and 1020 °C for 1 h in Argon gas protection and cooled down with the furnace in a natural way. To do the characterization, both the as-built samples and heat-treated ones were evaluated for microstructure, phases, and hardness by using analysis equipment including an X-ray diffractometer (XRD), optical microscope (OM), field emission-scanning electron microscope (SEM) and Vickers-Hardness tester.

Tab. 1: Parameter conditions of SLM process was used in this work.

Laser power (W)	Scan speed (mm/s)	Laser beam diameter (μm)	N_2	Hatch Distance (μm)	Layer thickness (μm)
120	1000	90	99.9 %	70	80

3 RESULTS AND DISCUSSION

Figs.1a and b present the optical microstructure and phase structures of the SLMed sample. It shows the typical microstructure of the SLMed sample with the dominance of the acicular martensitic α' at the top-view and the columnar grains which are identified as prior β grains containing the colonies of martensitic α' needles at the side-view. Furthermore, as examined in the SEM analysis, a high-resolution SEM image (Fig.2) reveals the microstructure of the SLMed sample consists of martensites α' in which the acicular laths cross on another and the grain boundary is hard to distinguish. There are some pores that is indicated by the black arrows.

The XRD patterns in Fig.1c exhibit only the primary α peaks for the initial powder, which are typical fingerprints of the hexagonal close-packed (hcp) structure of Ti without obvious peaks of the β phase indicating that the β-body-centered cubic grains fully transformed to α-hexagonal close-packed ones during the cooling stage of powder manufacturing. Similar characteristics of the XRD pattern are observed for the as-built sample. However, the peaks are sharper and the intensity of peaks in the case of the printed sample is higher than that of the powders. It is a fact that, the formation of α' martensite is due to the high cooling rate in the SLM process. According to previous studies [Ahmed 1998], the critical cooling rate of Ti-6Al-4V alloys for the formation of α' martensite in the microstructure is 104 K/s. However, the cooling rate in the SLM is approximately 683 K/s, significantly higher than that of the α′ martensite formation. Therefore, the formation of α′ martensite in the SLMed Ti-6Al-4V is not surprising.

For the heat-treated samples, their OM image is presented in the Fig.3a. At both side-view and top-view we could find out that they all have similar lamella microstructure including α and β phases. However, at the higher temperature heat treatment, the size of the lamellar is coarser. This result confirmed that the stabilizing of the lamellar microstructure (α+ β) for SLMed Ti-6Al-4V has been done by annealing at about 850 °C in 2.5 h; at 950 °C or 1020 °C in 1 hour followed by cooling naturally in the furnace. According to the literature, the conventional biomedical Ti-6Al-4V alloys usually show three distinct of microstructures that can be produced including lamellar, equiaxed, and bimodal structure [Peters 2003, Chen 2015, Virginia 2013, Rack 2015, Ahmed 1998]. These microstructures can be produced in Ti-6Al-4V through control of solution heat treatment temperature, cooling rate, and final aging temperature. The equiaxed alpha microstructures provide high strength and ductility and relatively low fracture toughness, whereas the lamella structure provides good fracture toughness, and the bimodal microstructure has the highest fatigue strength. In research [Rack 2015], H.J. Rack and J.I. Qazi reported that the lamellar structure is typically produced following heat treatment above the β transus temperature, followed by air cooling, and aging between 700 °C and 800 °C. Solution annealing below the β transus temperature, for example, between 800 °C and 925 °C results in an equiaxed structure. Finally, the bimodal structure may be developed by solution treatment below the β transus, typically between 900 °C and 950 °C followed by air cooling and aging below 700 °C. From these results and coming up with this work we can realize that after stabilizing lamellar microstructure (α+ β) by the solution heat treatment that this work has done, we can modify the microstructure by applying the aging step to control and achieve the other microstructure in the Ti-6Al-4V microstructure categories.

Fig. 3b presents the XRD pattern of the sample after heat treatment. The result shows that there are existence of the peaks corresponding to the α and β phases which is the difference to the XRD patterns of the Ti-6Al-4V powders and the as-built sample as well [Singla 2021, Ahmed 1998, Shugurov 2020]. This result also confirms the microstructure that has been discovered in the upper section of this study. The angle of the XRD peak (101) in the XRD pattern of the heat-treated Ti-6Al-4V sample is shifted to a lower diffraction angle than that of the sample produced by SLM in Fig.1c. This is interpreted to indicate a significant diffusion of V and Al in the Ti crystal structure.

An increase of interstitial or substituent atoms (Al) in the hcp lattice of Ti-6Al-4V alloy leads to a slightly increased c/a ratio of the α phase. All heat-treated samples exhibited an increase in the c/a ratio of the peak (101) compared with the SLMed sample. Moreover, in the SEM and EDS mapping analysis (Fig.4) it can be inferred that more V was dissolved in the β phase during the heat treatment as we can observe the distribution of about 7.7% V in the spectrum 5 (β-phase region) and about 2.0% V in the spectrum 6 (α-phase region).

The measured Vickers microhardness values of the 3D-printed Ti-6Al-4V samples before and after heat treatment are listed in Table 2. The hardness on the top-view (400 HV) and side-view (370 HV) of the as-printed sample is different, proving that the as-printed sample is anisotropic. The hardness value at the top- and side-view surface of heat-treated Ti6Al4V samples is quite similar at about 348 Hv and 343 Hv, respectively. This is smaller than the microhardness of the sample before heat treatment. It could be said that heat treatment results in the homogenization and stabilization of the hardness for the SLMed samples, and the change (reduction) in the hardness is attributed to the decomposition of α′ martensite into α and β phases.

Compared with conventional products such as cast and wrought parts [Pederson 2012, Shunmugavel 2015], the as-built sample achieves higher micro-hardness but it is not uniform and unstable. Thus, the as-built samples show a great variation in Vickers microhardness is about ~400 Hv and ~370 HV corresponding to the top-view and side-view, respectively. The micro-hardness of the 3D-printed Ti-6Al-4V after heat treatment reached an average of 346 HV which is in the range of 340 HV to 350 HV for the biomedical Ti-6Al-4V alloys [Niinomi 2008, Chen 2015, Virginia 2013, Önder 2023, Rack 2015]. This value is lower than that of the as-printed sample but uniform in the whole-body sample. And the most important thing here is the hardness value that the heat-treated Ti-6Al-4V samples achieved is stable as the result of the stress release process during heat treatment.

Tab. 2: Average micro-hardness of the specimens in the study.

Sample	**Hardness at the Top-view (HV)**	**Hardness at the Side-view (HV)**
SLMed	~400	~370
After Heat treatment	~348	~343
Conventional alloys [Pederson 2012, Shunmugavel 2015]	340-350	340-350

4 CONCLUSIONS

The solution heat treatments at 850, 950, and 1020 oC for the SLMed Ti-6Al-4V alloys have been done and successful in achievement of the uniform and stable microstructure as well as the hardness for the Ti-6Al-4V alloys. The stable microstructure was known as the lamella microstructure (α + β) phase which is suitable for application in medical implants. Come along with that microstructure, the hardness of the heat-treated alloy meets the suitable value for medical applications.

5 ACKNOWLEDGMENTS

This research was funded by Vietnam National Foundation for Science and Technology Development (NAFOSTED) under Grant Number 107.99-2018.336.

6 REFERENCES

[Singla 2021] Singla, A.K., et al. Selective laser melting of Ti6Al4V alloy: Process parameters, defects and post-treatments. Journal of Manufacturing Processes, 2021, Vol.64, pp 161-187.

[Niinomi 2008] Niinomi, M. Mechanical biocompatibilities of titanium alloys for biomedical applications. Journal of the Mechanical Behavior of Biomedical Materials, January 2008, Vol.1, No.1, pp 30-42.

[Peters 2003] Peters, M., Hemptenmacher, J., Kumpfert, J., Leyens, C. Structure and Properties of Titanium and Titanium Alloys, in Titanium and Titanium Alloys. Wiley Publisher, 2003. ISBN 9783527305346.

[Calignano 2019] Calignano, F., et al. Design of Additively Manufactured Structures for Biomedical Applications: A Review of the Additive Manufacturing Processes Applied to the Biomedical Sector. Journal of Healthcare Engineering, March 2019, Vol.2019, ID.9748212.

[Chen 2015] Chen, Q. and Thouas, G.A. Metallic implant biomaterials. Materials Science and Engineering: R: Reports, January 2015, Vol.87, pp 1-57.

[Virginia 2013] Virginia Sáenz de, V. and Elena, F. Titanium and Titanium Alloys as Biomaterials, in Tribology-Fundamentals and Advancement. London: IntechOpen Publisher, 2013. ISBN 978-953-51-1135-1.

[Nguyen 2020] Nguyen, M.T., et al. Properties of the interface between the as-built Ti–6Al–4V sample and the Ti substrate in selective laser sintering. International Journal of Modern Physics B. August 2020, Vol.34, No. 22n24, ID 2040137. ISSN 0217-9792.

[Önder 2023] Önder, S., Saklakoğlu N., and Sever, A. Selective laser melting of Ti6Al4V alloy: Effect of post-processing on fatigue life, residual stress, microstructure, microhardness and surface roughness. Materials Characterization. February 2023, Vol.196, ID 112571.

[Xu 2015] Xu, W., et al. Additive manufacturing of strong and ductile Ti–6Al–4V by selective laser melting via in situ martensite decomposition. Acta Materialia, February 2015, Vol.85, pp 74-84.

[Vilaro 2011] Vilaro, T., Colin, C., and Bartout, J.D. As-Fabricated and Heat-Treated Microstructures of the Ti-6Al-4V Alloy Processed by Selective Laser Melting. Metallurgical and Materials Transactions A, May 2011m Vol.42, pp 3190-3199.

[Pederson 2012] Pederson, R., Gaddam, R. and Antti, M.L. Microstructure and mechanical behavior of cast Ti-6Al-4V with addition of boron. Central European Journal of Engineering, April 2012, Vol.2, pp 347-357.

[Harun 2018] Harun, W.S.W., et al. A review of powder additive manufacturing processes for metallic biomaterials. Powder Technology, March 2018, Vol.327, pp 128-151.

[Rack 2015] Rack, H.J. and Qazi, J.I. Titanium alloys for biomedical applications. Materials Science and Engineering: C, September 2006, Vol.26, No.8, pp 1269-1277.

[Ahmed 1998] Ahmed, T. and Rack, H.J. Phase transformations during cooling in α+β titanium alloys. Materials Science and Engineering: A, March 1998, Vol.243, No.1, pp 206-211.

[Shugurov 2020] Shugurov, A.R., et al. Recovery of Scratch Grooves in Ti-6Al-4V Alloy Caused by Reversible Phase Transformations. Metals, October 2020, Vol.10, No.10, ID 1332.

[Shunmugavel 2015] Shunmugavel, M., Polishetty, A., and Littlefair, G. Microstructure and Mechanical Properties of Wrought and Additive Manufactured Ti-6Al-4V Cylindrical Bars. Procedia Technology, 2015, Vol.20, pp 231-236.

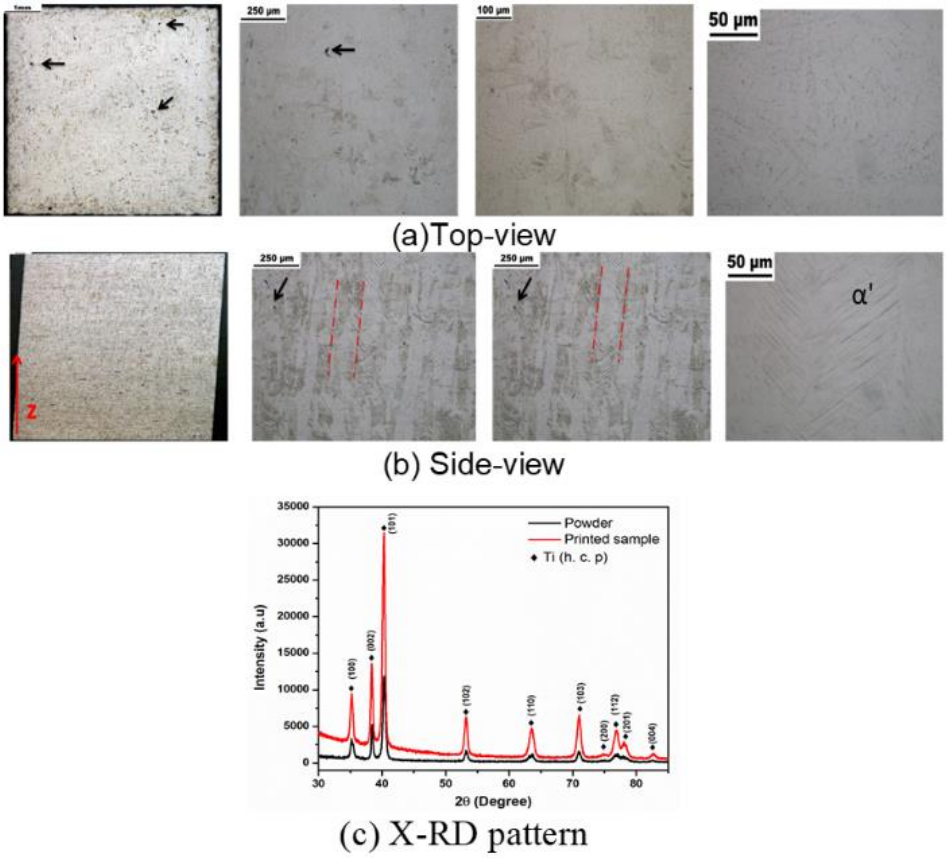

Fig. 1: Microstructure at the top-, side-view and XRD pattern of the SLMed sample.

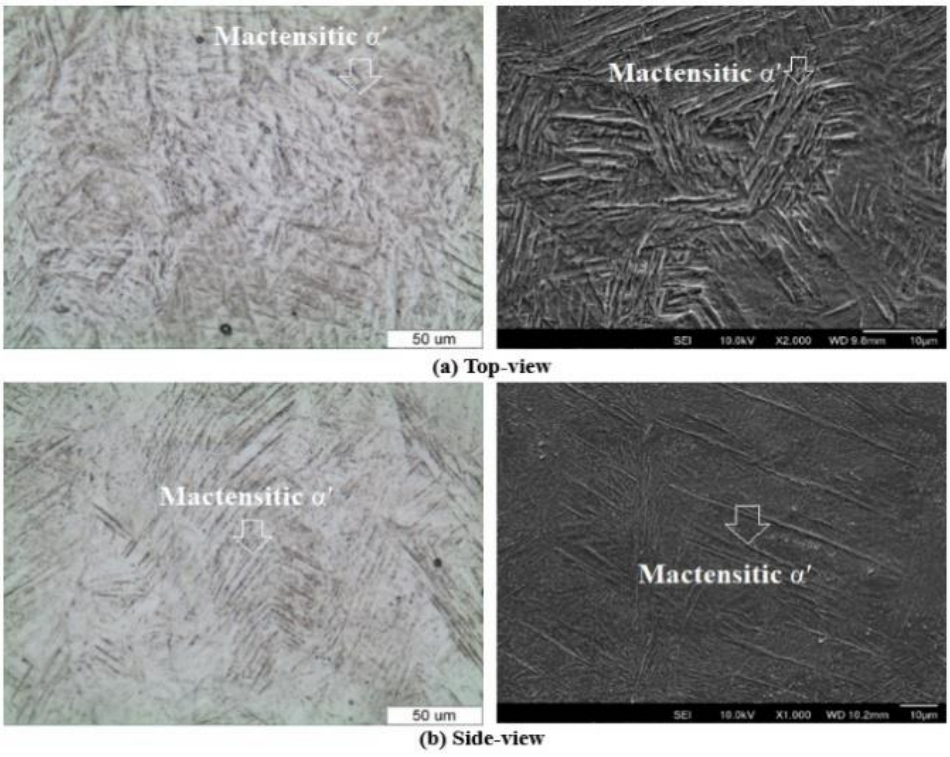

Fig. 2: OM and SEM images of printed Ti-6Al-4V sample.

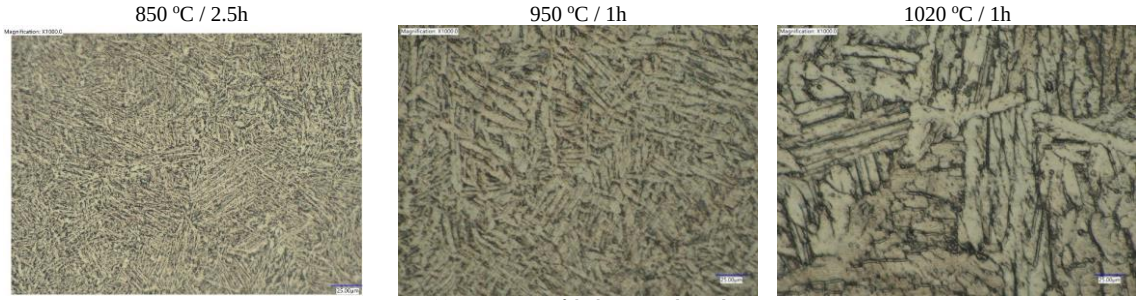

(a) OM images of the heat-treated samples

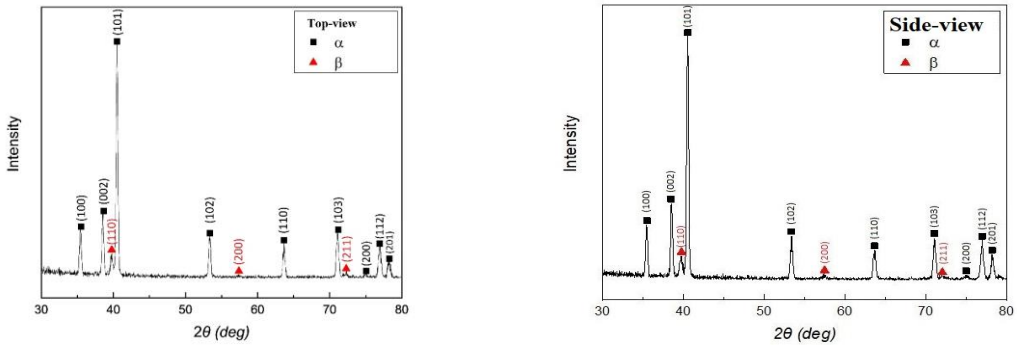

(b) XRD patterns of the heat-treated samples

Fig. 3: Microstructure and XRD pattern of the heat-treated sample.

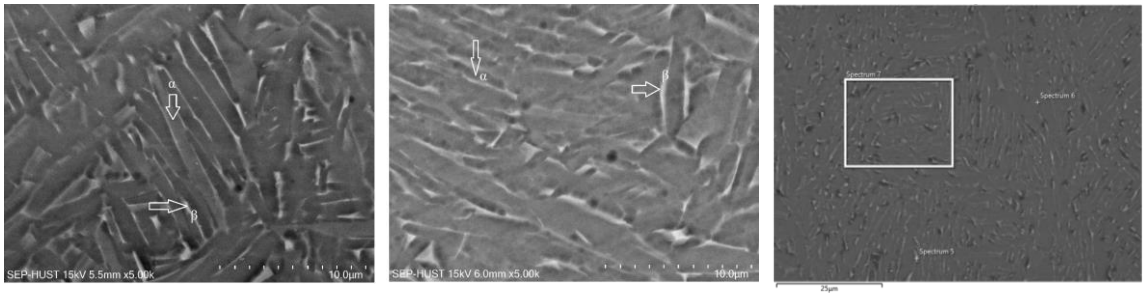

(a) SEM images

(b) EDS mapping

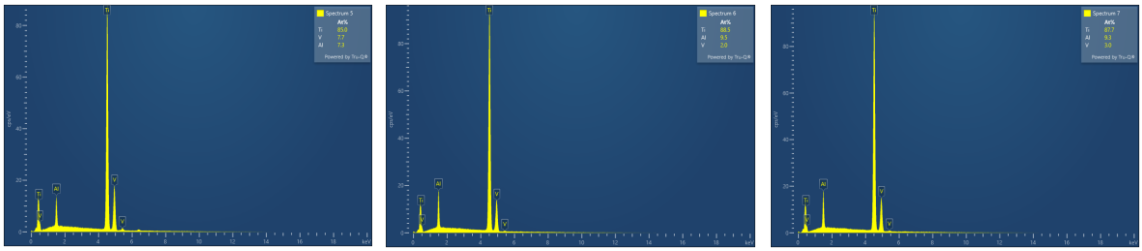

Fig. 4: SEM and EDS mapping images of the heat-treated sample.